Combining Photon Recycling and Concentrated Illumination in a GaAs Heterojunction Solar Cell

Claudia Lisa Schilling [ID], Oliver Höhn, Daniel Neves Micha [ID], Stefan Heckelmann, Vera Klinger, Eduard Oliva, Stefan W. Glunz [ID], *Senior Member, IEEE*, and Frank Dimroth [ID], *Member, IEEE*

Abstract—GaAs single-junction solar cells with rear-side-reflective structures have been developed aiming for an increase in open-circuit voltage V_{oc} by the combination of photon recycling and concentrated illumination of sunlight. Photon recycling gains importance with increasing sunlight concentration as the materials are increasingly dominated by radiative recombination. At the same time, resistive losses because of current transport must be addressed and minimized to achieve high performances. We report here on the development of a GaAs heterojunction solar cell which was optimized for operation under concentrated sunlight. An efficiency of 28.8% is achieved at 182 suns concentration, showing a V_{oc} of 1230 mV. This is an increase of 28 mV compared with a cell without a highly reflective back mirror. The results confirm the theoretically predicted positive effect of photon recycling under high concentration levels.

Index Terms—Concentrator photovoltaics, GaAs heterojunction solar cell, photon recycling, reflector.

I. INTRODUCTION

THE highest AM1.5 conversion efficiency of single-junction solar cells is reached with a GaAs absorber [1]. This is because of the nearly optimum bandgap energy for converting the different photon energies in the AM1.5 spectrum [2]. Furthermore, GaAs is a direct semiconductor with high internal luminescence efficiency. In other words, good GaAs structures are limited by radiative recombination already for incident intensities of 1000 W/m^2 or 1 sun [3]. Such solar cell devices benefit from photon recycling which has been widely discussed in the literature [4]–[8]. It has been found more recently that an important feature to maximize internal photon recycling is a rear-side reflector [4], [9], similar to what is used in modern light-emitting diodes (LEDs). This mirror reflects emitted photons back into the absorber layer and increases the probability of photon recycling. As a result, the open-circuit voltage V_{oc} is found to increase substantially for devices which incorporate efficient photon confinement and avoid parasitic absorption losses [4]. In fact, V_{oc} values up to 1.122 V at 1 sun have been reported for a GaAs single-junction solar cell with conversion efficiency of 28.8% ± 0.9% [1], [9] and of 29.3% ± 0.7% under a concentration of 49.9 suns [1].

In this work, we investigate how the GaAs solar cell structure has to be adapted for operation at high concentration levels up to 560 suns. Furthermore, we are studying the effect of photon recycling under concentration for a GaAs heterojunction cell fabricated on a GaAs bulk substrate or on a highly reflecting magnesium fluoride (MgF$_2$)/Ag back mirror. Here, one challenge is to realize a highly reflective mirror and simultaneously to create an excellent ohmic back contact that allows transporting high current densities under concentration. Current–voltage (*I–V*) characteristics are compared for both cell designs, confirming the importance of a highly reflective back mirror to reach high performance under concentrated irradiation.

II. SOLAR CELL DESIGN PRINCIPLES

One possibility to reduce radiative recombination losses and, thus, increase the open-circuit voltage of a GaAs single-junction solar cell is to enhance photon recycling. In general, emission of photons occurs in the semiconductor under all solid angles and the absolute probability of radiative recombination increases with the crystal quality. Emitted photons have a low probability for reabsorption, and therefore, it is important to ensure a sufficiently long pathway. This is achieved by reflecting the light several times between the front and rear of the solar cell structure. On the front side, the exit cone is determined by the high refractive index step from GaAs to air, resulting in an escape cone of around 16° which is not influenced by additional planar antireflective coatings. For angles greater than the critical angle (θ_c), total internal reflection occurs. This is schematically illustrated in Fig. 1.

However, on the rear side, emitted photons with all angles are usually transmitted into the GaAs substrate [see Fig. 1(a)] where parasitic absorption occurs. One possibility to decrease this loss is replacing the substrate by a mirror. According to simulation, V_{oc} increases superlinearly with increasing reflectivity of the mirror [4]. The increase is particularly pronounced for
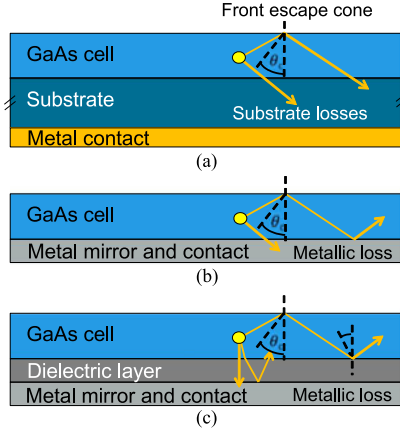
Fig. 1. Schematic cross section of solar cell on (a) substrate, (b) with a metallic mirror, and (c) with a dielectric layer between the photoactive layers and the metallic mirror.
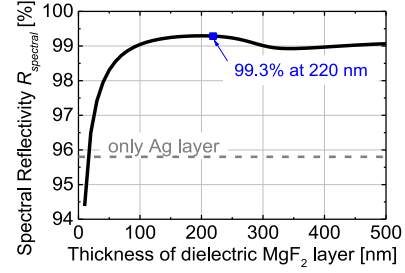

Fig. 2. Modeling of the spectral reflectivity R_{spectral} over the thickness of a dielectric MgF_2 layer. With a thickness of 220 nm, a maximal spectral reflectivity of 99.3% can be reached within the considered range of thicknesses up to 500 nm.

reflectivities above 95%. Therefore, it is of utmost importance to provide a mirror with high reflectivity to benefit from the nonlinear voltage boost.

The reflectivity is generally limited for metal mirrors [see Fig. 1(b)]. However, losses can be decreased by introducing an additional dielectric layer between the photoactive GaAs cell and the metal mirror [see Fig. 1(c)]. In this concept, total internal reflection at the semiconductor–dielectric interface occurs for all photons under angles larger than the critical angle. In addition, photons transmitted through the dielectric layer have a second chance for reflection at the metallic mirror. Parasitic absorption losses at the metal are reduced because of the smaller fraction of photons reaching the metal mirror. Of course, these losses are also highly dependent on the type of metal. This approach is similar to a passivated emitter and rear cell silicon solar cell [10]. Dielectric-metal stacks are also used in LED devices to increase the outcoupling efficiency [10].

We used silver as the metal because of its high reflectivity in the relevant wavelength regime for GaAs emission and magnesium fluoride as the dielectric coating. MgF_2 has a low refractive index in the range of 1.38–1.42 and, therefore, results in a high amount of total internal reflection. Any other dielectric with low refractive index would also be suitable.

III. THEORETICAL MODELING

A. Thickness of Dielectric Layer

The reflectivity of the mirror consisting of a dielectric and metallic layer depends on the thickness of the dielectric layer as interference effects occur in the thin film. The layer structure is modeled with the help of the transfer matrix formalism [12]. Here, the reflectivity of TE and TM polarization is averaged (R_{weighted}), integrated over all solid angles as shown in [13] and weighted with the emission spectrum E_m of GaAs (1). This reflectivity is labeled as spectral reflectivity R_{spectral}

$$R_{\mathrm{spectral}} = \frac{\int R_{\mathrm{weighted}} \cdot E_m}{\int E_m}. \tag{1}$$

MgF_2 was used as the dielectric layer and silver (Ag) as the metal. In Fig. 2, the spectral reflectivity is shown as a function of the thickness of the MgF_2 layer. In comparison, a pure silver mirror leads to a spectral reflectivity of 95.8%. For low MgF_2 thicknesses, the evanescent field in the dielectric layer prevents efficient total internal reflection. For MgF_2 layer, thicknesses up to 500 nm, a maximum spectral reflectivity of 99.3% is found for a thickness of 220 nm. Thus, a 220-nm-thick MgF_2 layer was used for the thin-film solar cells in this work.

B. Simulation of I–V Characteristics

The two-diode model given in (2) is used to model *I–V* curves. A detailed description of the model can be found in [14] and [15]

$$J(V) = J_{01}(V) + J'_{02}(V) + \frac{V - J \cdot R_S}{R_P} - J_{Ph} \quad \text{with}$$

$$J'_{01}(V) = J_{01} \cdot \left(\exp\left(\frac{q \cdot (V - J \cdot R_S)}{n_1 \cdot k_B T} \right) - 1 \right) \quad \text{and}$$

$$J'_{02}(V) = J_{02} \cdot \left(\exp\left(\frac{q \cdot (V - J \cdot R_S)}{n_2 \cdot k_B T} \right) - 1 \right). \tag{2}$$

This model considers the series (R_S) and parallel resistance (R_P) as well as the recombination current density in the diode (J_{01}) and in the depletion region (J_{02}). The temperature is assumed to be constant at $T = 298$ K; the bandgap energy is $E_G = 1.424$ eV for GaAs [16]. The ideality factors are assumed to be $n_1 = 1$ and $n_2 = 2$. The Boltzmann constant is given with k_B, the elementary charge with q, and the temperature with T. It is important to ensure that one set of parameters fits to all concentration-dependent *I–V* characteristics.

$J'_{01}(V)$ has an ideality factor of 1, $J'_{02}(V)$ an ideality factor of 2 which means that $J'_{01}(V)$ increases faster with voltage than $J'_{02}(V)$. The dark current of typical GaAs solar cells at 1-sun AM1.5g is influenced by both $J'_{01}(V)$ and $J'_{02}(V)$ whereas the $J'_{01}(V)$ term dominates for higher operating voltages under concentrated illumination. Radiative recombination is an important contribution to $J'_{01}(V)$, which decreases with increasing radiative efficiency (or in other words decreasing contribution of non-radiative recombination). Solar cells, in which radiative recombination is dominant and which have a back mirror, benefit from more photon recycling and consequently higher

external radiative efficiency. The external radiative efficiency (η_{rad}) can be calculated from (3) [17], where E is the energy, J_{sc} the short-circuit current density, h the Planck constant, and c the velocity of light. *External quantum efficiency* (*EQE*) can in good approximation be considered only for perpendicular incidence [18]

$$\eta_{rad} = \frac{\frac{2\pi q}{h^3 c^3} \cdot \exp\left(\frac{q \cdot V_{oc}}{k_B T}\right) \cdot \int_{E_G}^{\infty} \frac{\overline{EQE} \cdot E^2}{\exp(E/k_B T)-1} dE}{J_{sc}}. \quad (3)$$

From this, the concentration-dependent gain in V_{oc} because of enhanced photon recycling can be calculated as follows [19]–[21]:

$$\Delta V_{OC} = V_{OC}\,(\text{Mirror}, c) - V_{OC}\,(\text{Substrate}, c)$$
$$= \frac{k_B T}{q}\ln\left(\frac{\eta_{rad}\,(\text{Mirror}, c)}{\eta_{rad}\,(\text{Substrate}, c)}\right) \quad (4)$$

where V_{oc} (Mirror/Substrate, c) is the concentration (c)-dependent V_{oc} value for solar cell on substrate, respectively, on mirror. As mentioned above, the radiative efficiency increases with increasing concentration. This increase is—as also mentioned above—stronger for the cell with a rear-side mirror. Therefore, one can expect an increase in ΔV_{oc} with increasing concentration.

IV. EXPERIMENTAL REALIZATION

A. Epitaxial Growth of Solar Cell Structures

The solar cells are deposited by metal–organic vapor phase epitaxy on GaAs substrates. The cell design for the heterojunction structure is schematically shown in Fig. 3. The aluminum content increases from GaAs for the emitter up to $Al_{0.3}Ga_{0.7}As$ for the base. This epitaxial structure is used in order to reduce nonradiative recombination in the depletion region [22], [23]. Consequently, radiative recombination dominates, and the open-circuit voltage and the performance of the solar cell can be improved by enhanced photon recycling. Furthermore, a window layer and back surface field (BSF) are included to reduce minority carrier leakage and surface recombination losses.

Contact layers to achieve a low resistance semiconductor–metal contact are realized on the front and back side of the solar cell. Thin-film solar cells with a rear-side mirror required an additional etch stop layer for substrate removal and a lateral conduction layer for current transport under concentrated illumination.

B. Solar Cell Processing

The processing of solar cells started with the front-side technology. The highly doped contact layer was structured by photolithography and selective wet etching. A Ta_2O_5/MgF_2 antireflection coating and an ohmic front-side contact were deposited by e-beam and thermal evaporation, respectively. Subsequently, the cells on the wafer were separated electrically by photolithography and selective wet etching. In the next step, a sapphire wafer is temporarily bonded to the front side of the solar cell before removing the GaAs substrate in order to realize

n-GaAs	Contact layer	$5 \cdot 10^{18}$ cm^{-3}	400 nm
n-AlInP	Window	$9 \cdot 10^{18}$ cm^{-3}	25 nm
n-GaAs	Emitter	10^{17} cm^{-3}	2650 nm
p-Al$_x$Ga$_{1-x}$As			80 nm
p-Al$_{0.3}$Ga$_{0.7}$As	Base	10^{18} cm^{-3}	50 nm
p-Al$_{0.6}$Ga$_{0.4}$As	BSF	$2 \cdot 10^{18}$ cm^{-3}	70 nm
p-Al$_{0.1}$Ga$_{0.9}$As	Lateral conduction layer	$5 \cdot 10^{18}$ cm^{-3}	1400 nm
p-GaAs	Contact layer	$1.4 \cdot 10^{19}$ cm^{-3}	150 nm
p-GaInP	Etch stop	$2 \cdot 10^{18}$ cm^{-3}	200 nm
p-GaAs	Buffer	10^{18} cm^{-3}	325 nm
p-GaAs	Substrate	-	450 μm

Fig. 3. Schematic cross section of epitaxially grown GaAs heterojunction solar cell including doping and thickness of each layer. The aluminum content is increased up to 30% between emitter and base. BSF is the abbreviation for back surface field.

thin-film cells with rear-side mirror. Solar cell structures which remained on the substrate were finalized by the deposition of a back metal contact.

After the temporary stabilization, the GaAs substrate was removed by selective etching stopping on the GaInP etch stop layer, followed by a removal of this layer. Then, the contact layer on the back was structured by photolithography with a point contact mask and etched by selective wet etching. A dielectric MgF_2 layer with a thickness of 220 nm was evaporated thermally. A silver layer was sputtered as metallic mirror on top of the dielectric layer. Sputtering is used in order to achieve a good adhesion of Ag on MgF_2. After finishing the mirror, the back side contact was realized. For this purpose, the photoresist was lifted and an ohmic *p*-GaAs back contact (Pd/Zn/Pd/Au) was thermally evaporated. This back contact with point contacts through the dielectric layer covers only approximately 1% of the rear side. Finally, a thick copper layer was deposited by electroplating as conductive stabilization for the thin-film solar cells and the temporary bond on the front side was finally removed.

A schematic cross section of the solar cell structure is shown in Fig. 4; a photograph of a thin-film solar cell wafer with concentrator solar cells each having an area of 0.05367 cm^2 is shown in Fig. 5. For comparison, the same solar cell structure was also realized on a planar Ag mirror and on a conventional GaAs substrate.

V. RESULTS AND DISCUSSION

Thin-film solar cells with rear-side reflective structures have been characterized and compared with solar cells on substrate
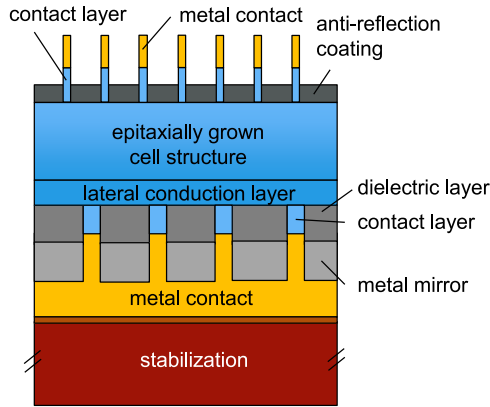
Fig. 4.   Schematic cross section of a thin-film solar cell with rear-side mirror consisting of a dielectric and metallic layer with point contacts.
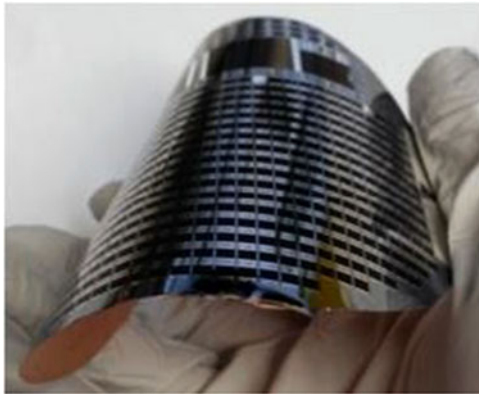

Fig. 5.   Photograph of a thin-film wafer with solar cells having a rear-side mirror. Such a thin-film wafer is around 34 μm thick, very flexible and lightweight.

Fig. 6.   Measured and modeled *I–V* characteristics of a solar cell on substrate and of a thin-film solar cell with a mirror consisting of an MgF$_2$ and Ag layer. The thin-film cell is measured under 182 suns, the cell on substrate under 177 suns. In the inset, the voltage range around the open-circuit voltage is enlarged.

TABLE I
PARAMETERS FOR MODELING *I–V* CURVES AT 298 K

Parameters	GaAs substrate	MgF$_2$ and Ag	Only Ag
J_{01} in mA/cm^2	$3 \cdot 10^{-17}$	$0.7 \cdot 10^{-17}$	$1.0 \cdot 10^{-17}$
J_{02} in mA/cm^2	$2.3 \cdot 10^{-8}$	$2.3 \cdot 10^{-8}$	$2.3 \cdot 10^{-8}$
R_p in $\Omega \cdot$ cm^2	$0.12 \cdot 10^6$	$0.12 \cdot 10^6$	$0.12 \cdot 10^6$
R_s in $\Omega \cdot$ cm^2	0.006	0.004	0.004

in order to show the open-circuit voltage increase because of the combination of photon recycling and concentrated illumination. For this purpose, *I–V* curves of the heterojunction solar cells with different rear-side reflector were measured under a flash based sun simulator up to 560 suns. The 1 sun (AM1.5d, ASTMG 173-03, 1000 W/m²) current of the devices has been determined at the calibration laboratory at Fraunhofer ISE including spectral mismatch correction. Some thin-film solar cells have a pure metallic Ag mirror and some feature a rear-side mirror consisting of a dielectric MgF$_2$ and a metallic Ag layer to achieve higher reflectivity. In Fig. 6, the measured *I–V* curves of a solar cell on substrate and of a thin-film solar cell with a back side mirror of MgF$_2$ and Ag are shown under 177 and 182 suns, respectively. The measured *I–V* curves are fitted using the two-diode model described in Section III. The modeling fits well to the measurement with parameters listed in Table I.

Regarding the fitting parameters, it becomes obvious that thin-film solar cells with a mirror on the rear side reach a lower recombination current density in the diode (J_{01}) compared with cells on substrate. This is attributed to the higher radiative efficiency as explained in Section III. This increase in V_{oc} can be seen in the *I–V* curves, especially in the inset of Fig. 6. Both series and parallel resistances are similar comparing solar cells
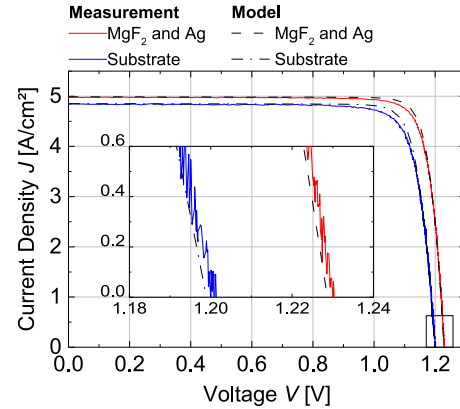
on substrate with thin-film cells with rear-side mirror. Moreover, for several concentration factors, *I–V* curves are recorded under concentrated illumination up to 560 suns. From these *I–V* curves, the open-circuit voltage V_{oc}, the fill factor FF, and the energy conversion efficiency η are extracted and weighted with the active area of the solar cell. In Fig. 7, these parameters are shown as a function of the logarithmic concentration. In addition, the measured V_{oc} values are listed in Table II, including the difference (Δ) between solar cells on substrate and thin-film solar cells with mirror.

V_{oc} increases logarithmically with increasing concentrated illumination. The V_{oc} values extracted from *I–V* curves simulated with the two-diode model (2) fit well to the measured V_{oc} both for solar cells on substrate and thin-film cells with reflector. This can be seen from the small difference between model and experimental results in Fig. 7.

The solar cells shown here are designed for operation under concentrated illumination. Nevertheless, 1-sun measurements are recorded as well. The values are listed in Table II. At 1 sun, the solar cells on substrate reach a V_{oc} of 1052 mV ($J_{sc} = 26.2$ mA/cm^2 and FF $= 85.4\%$). Thin-film architecture with a metallic silver mirror boosts the voltage by 20 to 1072 mV ($J_{sc} = 27.1$ mA/cm^2 and FF $= 85.8\%$). This is because of improved photon recycling. Moreover, the solar cell with a dielectric MgF$_2$ and silver mirror reaches a further increase in V_{oc} of 2 mV up to 1074 mV ($J_{sc} = 27.4$ mA/cm^2 and FF $= 87.1\%$). This is an increase of 22 mV compared with the cell on substrate. This voltage boost achieved with a dielectric
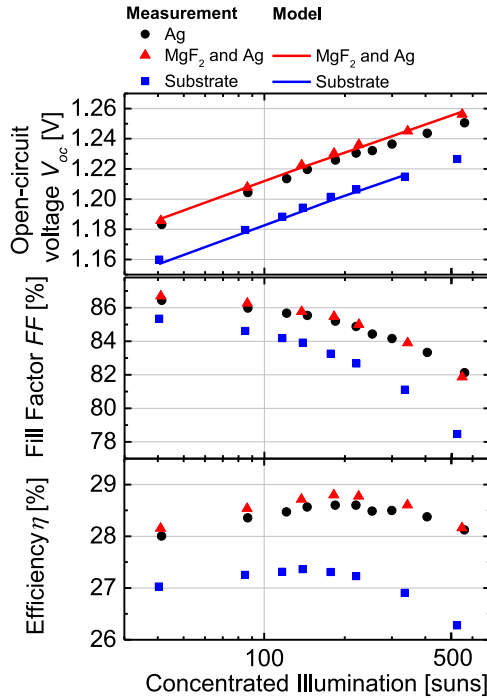
Fig. 7. Open-circuit voltage V_{OC}, fill factor FF, and energy conversion efficiency η as a function of the concentrated illumination for three GaAs heterojunction solar cells with a MgF$_2$/Ag mirror, a pure Ag mirror, and on substrate. All measurements were performed at 298 K.

Fig. 8. EQE for three GaAs heterojunction solar cells with a MgF$_2$/Ag mirror, a pure Ag mirror and on substrate.

TABLE II
OPEN-CIRCUIT VOLTAGES AND EXTERNAL RADIATIVE EFFICIENCY
FOR DIFFERENT CONCENTRATIONS

V_{oc} in mV	Concentration in suns	ΔV_{oc} in mV	η_{rad} in%	ΔV_{OC} expected from (4) in mV
GaAs substrate				
1052	1		2.5	
1202	177		4.5	
1226	526		n.a.	
Thin-film solar cell with Ag mirror				
1072	1	20	5	20
1226	184	24	11.2	24
1251	560	25	n.a.	n.a.
Thin-film solar cell with MgF$_2$/Ag mirror				
1074	1	22	5.3	20
1230	182	28	13.4	28
1258	556	32	n.a.	n.a.

The difference (Δ) compares open-circuit voltages of solar cells on substrate with thin-film solar cells on MgF$_2$/Ag mirror and on a pure Ag mirror of the values for η_{rad} were calculated from (3). Results for high concentrations are possibly affected by the serial resistance and therefore not shown.

layer between the photoactive layers and the metal mirror is expected since total internal reflection for photons with angles exceeding the critical angle can be reached. Photons with angles lower than the critical angle are still reflected at the metal. The V_{oc} difference between solar cells on substrate and with mirror is found to increase with concentration ratio. For the thin-film cell with silver mirror, an increase of 24 mV at 177 suns and of 25 mV at around 560 suns is realized. Furthermore, for the
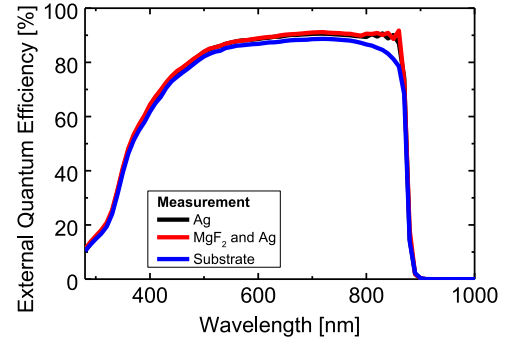
thin-film cells with MgF$_2$/Ag mirror, an increase in V_{oc} of 28 mV under 182 suns and of 32 mV under 556 suns is observed. This additional gain in V_{oc} for high concentration is—as shown in Section III-B—because of the fact that radiative recombination becomes even more dominant.

The lateral conduction layer is important for the thin-film devices with point contacts. No reduction in fill factor is observed up to high concentration levels which confirms that the lateral resistance is sufficiently low. A small gain in current is observed for the MgF$_2$/Ag cell compared with the cell Ag mirror. This can be seen from the quantum efficiency in Fig. 8.

The oscillations in the EQE close to the band gap are Fabry–Perot oscillations that occur because of interference of light reflected at the front and back surfaces. While the absorption is close to unity, the EQE is still significantly below 1. This is because of a small remaining reflection at the ARC, but more importantly because of metal grid shading of the concentrator solar cell device. The grid coverage has been designed for operation at high current densities and is a tradeoff between resistance losses and optical losses. This front metal grids results in approximately 8% absolute shading. This may be further reduced for cells operating at lower current densities.

The best GaAs heterojunction solar cell in this work has a reflector with a dielectric MgF$_2$ and metallic Ag layer and reaches a conversion efficiency of 28.8% with a V_{oc} of 1230 mV, a short-circuit current J_{sc} of 4.99 A/cm^2 and a fill factor of 85.5%. These values are achieved at 182 suns concentration of the AM1.5d, ASTMG 173-03 solar spectrum for a concentrator solar cell with an area of 0.05367 cm^2.

VI. CONCLUSION

We have investigated heterojunction GaAs solar cells under concentration, including different back side mirrors to enhance photon recycling. The best results were achieved for a cell with a rear-side reflector consisting of a dielectric MgF$_2$ and metallic Ag layer. Point contacts with an area <1% are formed to contact a highly doped Al$_{0.1}$Ga$_{0.9}$As layer which facilitates lateral conduction of majority carriers under concentration. Devices were measured up to high concentration levels of 560 suns. It was shown that the enhanced photon recycling in thin-film solar cells with back side mirror reduces the recombination

current density of the diode J_{01} and increases the V_{oc}. The best solar cell with MgF_2/Ag mirror exhibits a V_{oc} of 1230 mV at 182 suns which is an increase of 28 mV compared with cells on GaAs substrate. An energy conversion efficiency of 28.8% was measured for this device, close to the current record value of 29.3% $\pm$ 0.7% at 49.9 suns by LG [1]. Moreover, we have found that the gain in V_{oc} because of the rear-side mirror increases with the concentration ratio as radiative recombination becomes more dominant. This is in excellent agreement with the theoretical considerations in Section III-B, which are confirmed experimentally by our work.

ACKNOWLEDGMENT

REFERENCES

[1] M. A. Green *et al.*, "Solar cell efficiency tables (version 49)," *Prog. Photovolt. Res. Appl.*, vol. 25, no. 4, pp. 333–334, Jul. 2016, doi: 10.1002/pip.2855.

[2] W. Shockley and H. J. Queisser, "Detailed balance limit of efficiency of *p-n* junction solar cells," *J. Appl. Phys*, vol. 32, no. 3, pp. 510–519, Jun. 1961, doi: 10.1063/1.1736034.

[3] I. Schnitzer, E. Yablonovitch, C. Caneau, and T. J. Gmitter, "Ultrahigh spontaneous emission quantum efficiency, 99.7% internally and 72% externally, from AlGaAs/GaAs/AlGaAs double heterostructures," *Appl. Phys. Lett.,* vol. 62, no. 2, pp. 131–133, Oct. 1993, doi: 10.1063/1.109348.

[4] O. D. Miller, E. Yablonovitch, and S. R. Kurtz, "Strong internal and external luminescence as solar cells approach the Shockley–Queisser limit," *IEEE J. Photovolt.*, vol. 2, no. 3, pp. 303–311, Jun. 2012, doi: 10.1109/jphotov.2012.2198434.

[5] A. W. Walker *et al.*, "Impact of photon recycling on GaAs solar cell designs," *IEEE J. Photovolt.*, vol. 5, no. 6, pp. 1636–1645, Oct. 2015, doi: 10.1109/jphotov.2015.2479463.

[6] A. W. Walker *et al.*, "Impact of photon recycling and luminescence coupling on III–V single and dual junction photovoltaic devices," in *Proc. 42th IEEE Photovolt. Spec. Conf.*, New Orleans, LA, USA, Apr. 2015, pp. 14–19.

[7] A. Marti, J. L. Balenzategui, and R. F. Reyna, "Photon recycling and Shockley's diode equation," *J. Appl. Phys.*, vol. 82, no. 8, pp. 4067–4075, Jun. 1997, doi: 10.1063/1.365717.

[8] J. L. Balenzategui and A. Marti, "Detailed modelling of photon recycling: Application to GaAs solar cells," *Sol. Energy Mater. Sol. Cells*, vol. 90, nos. 7/8, pp. 1068–1088, May 2006, doi: 10.1016/j.solmat.2005.06.004.

[9] B. M. Kayes *et al.*, "27.6% Conversion efficiency, a new record for single-junction solar cells under 1 sun illumination," in *Proc. 37th IEEE Photovolt. Spec. Conf.*, Jun. 2011, pp. 000004–000008.

[10] D. Kray, M. Hermle, and S. W. Glunz, "Theory and experiments on the back side reflectance of silicon wafer solar cells," *Prog. Photovolt. Res. Appl.*, vol. 16, no. 1, pp. 1–15, May 2008, doi: 10.1002/pip.769.

[11] J. Q. Xi *et al.*, "Omnidirectional reflector using nanoporous SiO_2 as a low-refractive-index material," *Opt. Lett.*, vol. 30, no. 12, pp. 1518–1520, Jun. 2005, doi: 10.1364/OL.30.001518.

[12] B. Harbecke, "Coherent and incoherent reflection and transmission of multilayer structures," *Appl. Phys. B, Lasers Opt.*, vol. 39, no. 3, pp. 165–170, Jul. 1986, doi: 10.1007/BF00697414.

[13] O. D. Miller and E. Yablonovitch, "Photon extraction: The key physics for approaching solar cell efficiency limits," *Proc. SPIE*, vol. 8808, pp. 880807–880810, Sep. 2013, doi: 10.1117/12.2024592.

[14] P. Würfel, "Basic structure of solar cells," in *Physics of Solar Cells—From Principles to New Concepts*. Weinheim, Germany: Wiley-VCH, Dec. 2005, pp. 109–136, doi: 10.1002/9783527618545.ch6.

[15] O. Höhn, A. W. Walker, A. W. Bett, and H. Helmers, "Optimal laser wavelength for efficient laser power converter operation over temperature," *Appl. Phys. Lett.*, vol. 108, no. 24, Jun. 2016, Art. no. 241104, doi: 10.1063/1.4954014.

[16] M. Levinshtein, S. Rumyantsev, and M. Shur, "Gallium arsenide," in *Handbook Series on Semiconductor Parameters*, vol. 1. Singapore: World Scientific, 1996.

[17] M. A. Green, "Radiative efficiency of state-of-the-art photovoltaic cells," *Prog. Photovolt. Res. Appl.*, vol. 20, no. 4, pp. 472–476, Sep. 2012, doi: 10.1002/pip.1147.

[18] L. Ferraioli *et al.*, "Evidence for generalized Kirchhoff's law from angle-resolved electroluminescence of high efficiency silicon solar cells," *Appl. Phys. Lett.*, vol. 85, no. 13, pp. 2484–2486, Sep. 2004, doi: 10.1063/1.1795361.

[19] A. W. Walker *et al.*, "Nonradiative lifetime extraction using power-dependent relative photoluminescence of III-V semiconductor double-heterostructures," *J. Appl. Phys.*, vol. 119, no. 15, Apr. 2016, Art. no. 155702, doi: 10.1063/1.4945772.

[20] J. N. Munday, "The effect of photonic bandgap materials on the Shockley-Queisser limit," *J. Appl. Phys.*, vol. 112, no. 6, Sep. 2012, Art. no. 064501, doi: 10.1063/1.4742983.

[21] O. Höhn, "Winkelselektive Photonische Strukturen für eine Optimierte Strahlungsbilanz in Solarzellen: Solarzellen und optische Filter, Equation 4.10," Ph.D. dissertation, Technische Fakultät, Fraunhofer-Institut für Solare Energiesysteme ISE, Albert-Ludwigs-Universität, Freiburg im Breisgau, Germany, Jul. 2014.

[22] S. Heckelmann, D. Lackner, C. Karcher, F. Dimroth, and A. W. Bett, "Investigations on $Al_x Ga_{1-x} As$ solar cells grown by MOVPE," in *Proc. 40th IEEE Photovolt. Spec. Conf.*, Denver, CO, USA, Jun. 2014, pp. 446–453.

[23] S. T. Hwang *et al.*, "Bandgap grading and $Al_{0.3}Ga_{0.7}As$ heterojunction emitter for highly efficient GaAs-based solar cells," *Sol. Energy Mater. Sol. Cells*, vol. 155, pp. 264–272, Oct. 2016, doi: 10.1016/j.solmat.2016.06.009.

Claudia Lisa Schilling was born in Balingen, Germany, in 1992. She received the Bachelor's degree in 2014 and M.Sc. degrees in microsystems engineering from Albert-Ludwigs-University, Freiburg, Germany, in 2017, with a thesis on "The development of highly reflective contact layers for III-V concentrator solar cells."

Since 2015, she has been a Student Assistant with the Group "III-V Semiconductor Technology", Fraunhofer Institute for Solar Energy Systems ISE, Freiburg. Her main focus is based on the technological realization of thin-film GaAs concentrator solar cells with back side mirror.

Oliver Höhn received the Diploma and Ph.D. degrees from Albert-Ludwigs-University, Freiburg, Germany, in 2011 and 2015, respectively, both in physics, with a thesis on "Winkelselektive photonische Strukturen für eine optimierte Strahlungsbilanz in Solarzellen."

He joined the Fraunhofer Institute for Solar Energy Systems ISE, Freiburg, in 2008. His main research interests include III–V multijunction solar cells, optical modeling and realization of micro- and nanostructured surfaces and optical modeling of high-efficiency solar cells.

Daniel Neves Micha, photograph and biography not available at the time of publication.

Stefan Heckelmann, photograph and biography not available at the time of publication.

Vera Klinger was born in Hamburg, Germany, in 1982. She received the Diploma degree in physics from RWTH Aachen, Aachen, Germany, in 2007, the M.B.A. degree in 2008 from the Technical University of Aachen (RWTH), and the Ph.D. degree in physics from the University of Konstanz, Konstanz, Germany, in 2013, with a thesis on "The development of ultra-thin multijunction solar cells for the achievement of highest efficiencies."

She joined the Fraunhofer Institute for Solar Energy Systems ISE, Freiburg, Germany, in 2008, and has been leading the Group "III-V Semiconductor Technology" with the division "Photovoltaics" at Fraunhofer ISE since 2014. Her main research interests include the III–V multijunction solar cell manufacturing technology for space and terrestrial applications as well as novel cell concepts with integrated interconnections.

Eduard Oliva was born in Nowokusnezk, Russia, in 1977. He received the Engineering degree in microelectronics from the University of Nowotscherkassk, Nowokusnezk, in 1999, and the Ph.D. degree in semiconductor technology from the University of Nowotscherkassk in cooperation with the Photovoltaics Laboratory, Ioffe Physico-Technical Institute, St. Petersburg, Russia, in 2002.

Since October 2005, he has been an Engineer with the "III-V—Epitaxy and Solar Cells" Department, Fraunhofer Institute for Solar Energy Systems ISE, Freiburg, Germany. His main research interest includes the development of process technologies for the fabrication of high-efficiency III–V photovoltaic converters.

Stefan W. Glunz (M'10–SM'14) received the Ph.D. degree (physics) from the University of Freiburg, Freiburg, Germany, in 1995.

He is the Director of the "Solar Cells—Development and Characterization" Division, Fraunhofer Institute for Solar Energy Systems, Freiburg, and a Professor with the Laboratory of Photovoltaic Energy Conversion, Albert-Ludwigs-University, Freiburg. He is the author/coauthor of more than 100 journal papers in the field of photovoltaics. His research interests include the design, fabrication, and analysis of high-efficiency solar cells.

Dr. Glunz is the Founding Editor for IEEE JOURNAL OF PHOTOVOLTAICS. In 2008, he received the Eni Award for the promotion of science and technology in the field of renewable energies and in 2014 the Becquerel Award for Outstanding Merits in Photovoltaics.

Frank Dimroth (M'13) received the Diploma degree from the University of Zurich, Zürich, Switzerland, in 1996, and the Ph.D. degree from the University of Konstanz, Konstanz, Germany, in 2000, both in physics.

He is the Head of the Department "III-V Epitaxy and Solar Cells" with the Fraunhofer Institute for Solar Energy Systems, Freiburg, Germany. His department carries out applied research in the fields of III–V multijunction solar cells and concentrator photovoltaic systems. He developed space and concentrator solar cells with efficiencies up to 46% at 500 suns. He has published more than 200 scientific papers and 15 patents in this field.

Dr. Dimroth and his team received the Fraunhofer Prize in 2010, the French Louis D Science Award in 2010, and the French-German Economy Prize in 2011. He is an Editor for IEEE JOURNAL OF PHOTOVOLATICS in the field of III–V concentrator, and space photovoltaic.